

KfK 4695
IKE 6-180
März 1990

Calculation of the Benchmark 20 of the OECD-NEA Working Group on Criticality Calculations

W. Bernnat, J. Keinert

**Institut für Neutronenphysik und Reaktortechnik
Institut für Kernenergetik und Energiesysteme, Stuttgart**

Kernforschungszentrum Karlsruhe

KERNFORSCHUNGSZENTRUM KARLSRUHE

Institut für Neutronenphysik und Reaktortechnik
Institut für Kernenergetik und Energiesysteme, Stuttgart

KfK 4695
IKE 6-180

Calculation of the Benchmark 20 of the
OECD-NEA Working Group on Criticality Calculations*

Wolfgang Bernnat, Jürgen Keinert

Postal address: IKE, Pfaffenwaldring 31, D-7000 Stuttgart 80

* This work was funded by the Kernforschungszentrum Karlsruhe GmbH,
Federal Republic of Germany

Als Manuskript vervielfältigt
Für diesen Bericht behalten wir uns alle Rechte vor

Kernforschungszentrum Karlsruhe GmbH
Postfach 3640, 7500 Karlsruhe 1

ISSN 0303-4003
ISSN 0173-6892

Abstract

The benchmark 20 is a hypothetical criticality problem consisting of 2.5 % enriched UO₂ spherical pellets in borated water or borated water UO₂ slurries. The volume fraction of the pellet to the slurry, the boron concentration, and the fraction of the total UO₂ in the slurry were varied. The main problem of this benchmark is the adequate treatment of resonances in the zone with borated water and UO₂ slurries. The criticality calculations for the benchmark were performed by means of the program system RSYST/CGM based on JEF-1 data. The neutron spectrum in the range of resolved resonances of U-238 (4 keV - 3 eV) was calculated by solving the slowing down equation for a large number of groups (lethargy-width 0.001) for a multicone-cell (first-collision P^k-method). The dependency of the neutron spectrum and the weighted cross-sections in the resonance range will be shown as a function of the UO₂ fraction in borated water for the pitches with UO₂ volume fractions 0.4 and 0.6 respectively. k-infinity was calculated for all variations with a 1D-cell-model in spherical geometry (white boundary conditions). The effect of the square pitch and triangular pitch was studied with a transport method (127 energy groups) based on 3D first-collision probabilities calculated by Monte Carlo. The results of these calculations show a very good agreement with a solution of CEA (CEA reference solution based on APOLLO/PIC and the CEA 86 library).

Berechnung des Benchmarks Nr. 20 der OECD-NEA-Arbeitsgruppe über Kritikalitätsrechnungen

Kurzfassung

Das Benchmark Nr. 20 ist ein hypothetisches Kritikalitätsproblem, das aus einem regelmäßigen Gitter von kugelförmigen Pellets aus 2,5 % angereichertem UO₂ in boriertem Wasser oder boriertem Wasser mit aufgelöstem UO₂ besteht. Das Volumenverhältnis von Pellets und umgebender Lösung, die Borkonzentration und der Anteil des UO₂ in der Lösung werden variiert. Das wesentliche Problem dieses Benchmarks ist die Resonanzbehandlung für den Fall, daß UO₂ nicht nur in der Pellet-Zone, sondern auch in der umgebenden Zone vorhanden ist. Die Kritikalitätsrechnungen für dieses Benchmark-Problem wurden mit Hilfe des Programmsystems RSYST/CGM auf der Basis von JEF-1-Daten durchgeführt. Das Neutronenspektrum im Bereich der aufgelösten Resonanzen des U-238 (4 keV - 3 eV) wurde durch Lösung der Bremsgleichung für eine große Zahl von Energiegruppen (Lethargiebreite 0,001) für ein Multizonen-Modell nach der Erststoß-P^k-Methode berechnet. Die Abhängigkeit des Neutronenspektrums und der Multigruppenquerschnitte vom Anteil des UO₂ in boriertem Wasser wird für zwei Gitterweiten mit den UO₂-Volumenanteilen 0,4 und 0,6 gezeigt. Für alle spezifizierten Fälle des Benchmark-Problems wurde k-unendlich für ein sphärisches Zellmodell (mit weißer Randbedingung) berechnet. Der Einfluß eines quadratischen bzw. dreieckförmigen Gitters wurde mit einer Erststoßmethode (127 Energiegruppen) untersucht, bei welchen die 3D-Stoßwahrscheinlichkeiten mit der Monte-Carlo-Methode bestimmt wurden. Die Ergebnisse der Benchmark-Rechnungen zeigen eine sehr gute Übereinstimmung mit einer Lösung von CEA, die mit APOLLO/PIC und der CEA86-Bibliothek berechnet wurde.

Contents

	Page
Introduction	1
Calculation Method	1
Data Base	1
Spectral Calculation	2
Lattice Calculations	2
K_{eff}-Calculation	2
Results	3
Comparison of other Solutions	4
Conclusions	4
References	6
Acknowledgement	7
Tables and Figures	8
Annex	29

List of Figures and Tables

Table 1: k_{inf} and k_{eff} for benchmark exercise 20 (3500 ppm Boron)

Table 2: k-infinity and $\Delta\rho$ values for benchmark exercise 20

Table 3: Exercise 20: Case 1b

Table 4: Exercise 20: Case 3b

Table 5: Exercise 20: Case 1f

Table 6: Exercise 20: Case 3f

Figure 1: Generation of multigroup cross-section libraries for calculation of thermal fission systems

Figure 2: The RSYST/CGM module for cross-section processing for thermal reactor calculations

Figure 3: Geometry for tetraedric cell (z-plane)

Figure 4: k-infinity for the Benchmark 20 as a function of UO_2 in pellets (CGM/JEF-1)

Figure 5: k-infinity for the Benchmark 20 as a function of UO_2 volume fraction (CGM/JEF-1)

Figure 6: Relation between weighted U-238 multigroup-absorption cross-sections (GAM-II + LASER structure) for 25 %, 50 %, 75 % and 100 % UO_2 in pellet and cross sections for the homogeneous case (0 %)

Figure 7: Relation between weighted U-238 multigroup-absorption cross-sections (GAM-II + LASER structure) for 25 %, 50 % and 75 % UO_2 in pellet and cross-sections for the homogeneous case (0 %)

Figure 8: Relation between weighted U-238 multigroup-absorption cross-sections (GAM-II + LASER structure) for 25 %, 50 % , 75 % and 100 % UO_2 in pellet and cross-sections for the homogeneous case (0 %)

Figure 9: Relation between weighted U-238 multigroup-absorption cross-sections (GAM-II + LASER structure) for 25 %, 50 % and 75 % UO_2 in pellet and cross-sections for the homogeneous case (0 %)

Figure 10: Neutron flux spectra in the pellet and water zone ($10\% UO_2$, $vf = 0.4$, 1500 ppm)

Figure 11: Neutron flux spectra in the pellet and water (+ UO_2) zone ($50\% UO_2$, $vf = 0.4$, 1500 ppm)

Figure 12: Neutron flux spectra in the pellet and water (+ UO_2) zone ($100\% UO_2$, $vf = 0.6$, 1500 ppm)

Figure 13:Neutron flux spectra in the pellet and water (+ UO₂) zone (50 % UO₂, vf = 0.6, 1500 ppm)

Figure 14:Neutron flux spectra as a function of pellet remaining (vf = 0.4, 1500 ppm, pellet zone)

Figure 15:Neutron flux spectra as a function of pellet remaining (vf = 0.4, 1500 ppm, moderator zone)

Figure 16:Neutron flux spectra as a function of pellet remaining (vf = 0.6, 1500 ppm, pellet zone)

Figure 17:k-infinity as a function of the pellet dissolution

Figure 18: Δp as a function of the pellet dissolution

Figure 19:k-eff/k-infinity ratios for the Benchmark 20

Introduction

The benchmark 20 (specification given in annex) represents a problem with double heterogeneity. The main problem is the calculation of self-shielded cross-sections in the region with borated water and UO_2 slurries which is often not accurately possible using standard spectral codes. However, if the resonance treatment is not adequate in this region - which cannot be treated separately from the neighbouring UO_2 -pellet region of the lattice - the reactivity loss due to the solved UO_2 in the borated water may be overestimated. Therefore for the calculation of the benchmark a method was used which solves the neutron slowing down equation for both UO_2 -pellet and borated water UO_2 -zone simultaneously using a sufficiently large number of neutron groups to resolve the most important resonances of U-238 (lethargy-width 0.001). Using this method we had good experiences for a large number of benchmarks [1] and reactor calculations [2].

Calculation Method

Data Base

The calculations are based on multigroup libraries derived from the JEF-1 evaluated data file [3]. For the generation of the multigroup libraries the NJOY nuclear data processing system [4] was used. These libraries consist in three separate sections (Fig. 1):

- the 'thermal' library for the energy range from 10^{-5} to 3.059 eV with 151 groups;
- the 'fast' library for the fast and epithermal energy range from 0.414 eV to 14.98 MeV with 99 groups in GAM-II structure;
- the 'resonance' library for the energy region from 0.876 eV to 4.3 keV with 8500 groups.

The tolerance used for reconstructing the resonance cross-sections and for Doppler broadening in NJOY was 0.1 percent.

Spectral Calculation

For the calculation of the requested quantities of the benchmark 20 (k -infinity for an infinite cubic or triangular lattice and k -effective for an infinite cylinder of 20 cm radius) problem dependent broad group data were calculated by the spectral program CGM [5]. CGM calculates spectra for fast, resonance and thermal energy range using the corresponding multigroup libraries. The cell model used in CGM was a 1D-spherical multizone model with white boundary conditions at the outer boundary. A flow-chart of CGM shows Fig. 2. For every zone of the cell resonance nuclides may be specified together with moderator or structural materials. The main module of CGM is the part with the spectral calculation for the resonance range for the hyperfine groups. This part is based on the P^{ik} -slowing down code RESAB-2 [6]. This part guarantees an adequate solution of the problem also if resonance nuclides are present in the moderator zone. In this range the code uses correctly calculated first-collision probabilities (no Bondarenko method).

Lattice Calculations

By means of CGM-calculations 127 group cross-sections were generated (91 groups in GAM-II structure, 36 groups in LASER structure) for all variations of the benchmark. With the cell homogenized macroscopic cross-sections k_{eff} -calculations with ANISN [7] (127 groups, S_6-P_1 -approximation) were performed as well as k -infinity calculations for the lattice. As lattices a cubic lattice and a hexagonal lattice (see benchmark specification in the annex) was regarded. CGM uses a 1D-cell model which cannot differentiate between the two lattice types. Therefore the modules RAWCOL/ISORCB [8] of the modular program system RSYST [9] were used to solve the transport equation for the correct lattice geometries using first-collision probabilities calculated by a Monte-Carlo-method implemented in RAWCOL (see Fig. 3, geometry for the hexagonal lattice).

These calculations were also performed with 127 groups.

k_{eff} -calculations

Macroscopic homogenized cell cross-sections calculated by the spectral code CGM were used for k_{eff} -calculations for an infinite water reflected cylinder (radius 20 cm, reflector thickness 30 cm) by the S_N -transport program ANISN. 127 groups P_1 -data and S_6 -order were used in ANISN. The geometrical model is specified in the annex too.

Results

The results of the calculations - k_{infinity} and k_{eff} for pellet diameters 0.96 cm (full); 0.872 cm (3/4); 0.762 cm (1/2), boron levels 3500 and 1500 ppm and square pitches of 0.5; 0.4 UO_2 volume fractions as well as triangular pitches of 0.6; 0.5 and 0.4 UO_2 volume fractions - are listed in Tab. 1. In this table the results of 1D-cell calculations for the 0.6; 0.5 and 0.4 UO_2 volume fractions are listed in the columns for the hexagonal lattice (but regard that the 1D-model cannot differentiate between the two lattice types).

The results of the 3D-cubic and hexagonal cell-calculations are listed in Tab. 1 too.

The k_{eff} -values listed in Tab. 1 are calculated with homogenized cell cross-sections taken from the 1D-cell calculations. A comparison of k_{infinity} calculated by the 1D-cell model and the cubic and dodecahedral cell model shows that the spherical 1D-cell model with white boundary conditions represents the realistic lattices sufficiently. The error is less than 0.2 %.

The k_{infinity} -values listed in Tab. 1 are plotted as a function of the fraction of UO_2 in pellets in Fig. 4 (1D-cell-calculations). From Fig. 5 one can see that the system is nearly optimally moderated for the vf-rate of 0.5 in the 1500 ppm case but under-moderated for the 3500 ppm cases (vf-rate 0.4 - 0.6).

The dependency of the microscopic (127) multigroup-absorption cross-sections of U-238 from the different UO_2 -volume fraction rates and UO_2 -densities in the borated water zones are shown in Fig. 6 (vf = 0.4, 1500 ppm, pellet-zone), Fig. 7 (vf = 0.4, 1500 ppm, moderator + UO_2 -zone), and for vf = 0.6 in Fig. 8 and Fig. 9, respectively. For every different case the slowing down equation was solved for the hyperfine group structure in the resonance range. The self-shielding effects can be seen from these figures. An impression of the flux-spectra in the pellet and water(+ UO_2)-zone shows Fig. 10 for 100 % UO_2 in pellets (vf = 0.4, 1500 ppm), and Fig. 11 correspondingly for 50 % UO_2 in pellets. Fig. 12 and Fig. 13 show the spectra for the vf = 0.6 rate. In Fig. 14 the flux density in the resonance range is shown as a function of energy and remaining fraction of UO_2 in pellets (flux density in pellets, vf = 0.4), a corresponding plot is shown in Fig. 15 for the flux density in the water + UO_2 -zone. Fig. 16 shows the corresponding curve for the pellet zone with vf = 0.6. For the moderator zone with vf = 0.6 the results are similar to those of Fig. 15.

From these figures the complicated dependency of the resonance fluxes in pellet and water + UO_2 -zones can be seen. For reliable criticality calculations, it is necessary to take into account these dependency for the generation of problem dependent multigroup cross-sections and calculation of integral parameters such as reaction rates and k-effective.

Comparison to other Solutions

For comparisons with other solutions the cases $vf = 0.6$ and 0.4 , 1500 ppm (100% , 75% , 50% , 25% and 0% remaining pellets) are listed in Tab. 2 together with a solution of CEA (based on APOLLO/PIC and CEA 86 library) presented at a working group meeting in June 1989.

For further comparisons reaction rates for the main nuclides are given in the Tab. 3 - 6 for the 1500 ppm cases 1b (100% UO_2 in pellet, UO_2 cell fraction 0.6), 3b (100% UO_2 in pellet, UO_2 cell fraction 0.4), 1f (50% UO_2 in pellet, 50% in solution, UO_2 fraction in H_2O 0.429), and 3f (50% UO_2 in pellet, 50% in solution, UO_2 fraction in H_2O 0.25). The normalization of rates in these tables is such that the total absorption is 1.0016 for the $vf = 0.4$ cases and 1.0024 for the $vf = 0.6$ cases (the deviations from 1.0000 account for the $n,2n$ production). For the most important nuclides, the agreement with the CEA-reference values is very good. A comparison of k-infinity as a function of remaining pellet volume is shown in Fig. 17. In Fig. 18 the corresponding $\Delta\rho$ -values (reactivity loss) are shown (definition: $\Delta\rho = (k_2 - k_1)/(k_1 \cdot k_2)$).

Finally the k-eff/k-infinity ratio is shown in Fig. 19.

The values based on the CGM/JEF-1 calculations agree well with the CEA/APOLLO solution. No discrepancies larger than a few permille were found for all compared cases (also the 25% cases and 0% cases which were not defined in the original benchmark description). It seems that the methods are comparable. An important fact is that the solutions converge against the homogeneous case which can be easily calculated by all standard codes.

Conclusions

The benchmark 20 must be calculated with a method which takes into account the correlation between spectra in pellet and the moderator + UO_2 -zone. The three-dimensional

lattice may be treated by a 1D-cell model with white boundary conditions without remarkable errors. Of course the data base itself plays an important role. From the comparison with the CEA-solution (also for the standard cases: homogeneous and no UO_2 in moderator) one can conclude that our calculations based on JEF-1 and CGM agree well with CEA-solutions in the range which is covered by this benchmark.

References

- [1] Bernnat, W.; Mattes, M.; Arshad, M.; Emendörfer, D.; Keinert, J.; Pohl, B.: Analysis of Selected Thermal Reactor Benchmark Experiments Based on the JEF-1 Evaluated Nuclear Data File.
Stuttgart: IKE, 1986 (IKE 6-157, JEF Report 7)
- [2] Lutz, D.; Bernnat, W.; Mattes, M.:
DWR-Zyklusrechnungen auf der Basis von JEF-1 und ENDF/B-IV/V.
Jahrestagung KERNTECHNIK '90, 71 (1989), 9.-11.5.1989, Düsseldorf
- [3] Rowlands, J.L.; Tubbs, N.:
The Joint Evaluated File: A New Nuclear Data Library for Reactor Calculations.
Int. Conf. Nuclear Data for Basic and Applied Science, Santa Fé, USA, Vol. 2 (1985), 1493
- [4] MacFarlane, R.E.; Muir, D.W.; Boicourt, R.M.:
The NJOY Nuclear Data Processing System.
LA-9303, Vol. I-III (1982-1987)(ENDF-324)
- [5] Arshad, M.:
Entwicklung und Verifikation eines Programmsystems zur Berechnung von Spektren und gewichteten Gruppenkonstanten für thermische und epithermische Spaltstoffsysteme.
Stuttgart: IKE, 1986 (IKE 6-156)
- [6] Riik, B.; Rühle, R.:
RESAB2, ein Programm zur Berechnung von Gruppenkonstanten im Resonanzbereich nach der Stoßwahrscheinlichkeitsmethode.
Stuttgart: IKE, 1972 (IKE 3.3-6.129)
- [7] Engle, W.W., Jr.:
A User's Manual for ANISN, a One-Dimensional Discrete Ordinates Transport Code with Anisotropic Scattering.
ORNL K-1693 (1967)
- [8] Neumann, K.:
RAWCOL, ein Programmsystem zur Berechnung von Stoßwahrscheinlichkeiten für beliebige Geometrien.
Stuttgart: IKE, internal report
- [9] Rühle, R.:
RSYST, ein integriertes Modulsystem mit Datenbasis zur automatisierten Berechnung von Kernreaktoren.
Stuttgart: IKE, 1973 (IKE 4-12)

Acknowledgement

The authors like to thank to Dr. Küsters of the Institute of Neutron Physics and Reactor Technology (INR) for the kind support of this work.

Tables and Figures

Table 1 : k_{inf} and k_{eff}
for Benchmark Exercise 20 (3500 ppm Boron)

100% UO_2 in pellets : $d = 0.96$ cm

	Triang. Pitch			Square Pitch	
	VF = 0.6 1 a	VF = 0.5 2 a	VF = 0.4 3 a	VF = 0.5 4 a	VF = 0.4 5 a
1D-Cell *) k_{inf}	1.0102	0.9955	0.9360		
3D-Cell k_{inf}	1.0099	-	0.9443	0.9930	0.9337
ANISN **) k_{eff}	0.7926	0.7871	0.7459		

75% UO_2 in pellets : $d = 0.872$ cm

	Triang. Pitch			Square Pitch	
	VF = 0.6 1 c	VF = 0.5 2 c	VF = 0.4 3 c	VF = 0.5 4 c	VF = 0.4 5 c
1D-Cell *) k_{inf}	0.9924	0.9744	0.9140		
3D-Cell k_{inf}	0.9918	-	0.9166	0.9732	0.9127
ANISN **) k_{eff}	0.7775	0.7707	0.7302		

50% UO_2 in pellets : $d = 0.762$ cm

	Triang. Pitch			Square Pitch	
	VF = 0.6 1 e	VF = 0.5 2 e	VF = 0.4 3 e	VF = 0.5 4 e	VF = 0.4 5 e
1D-Cell *) k_{inf}	0.9874	0.9704	0.9119		
3D-Cell k_{inf}	0.9881	-	0.9142	0.9699	0.9113
ANISN **) k_{eff}	0.7726	0.7671	0.7284		

*) values not dependent from lattice geometry

**) homogenized cell cross-sections from the 1D-Cell calculations are used

Table 1 continued :
(1500 ppm Boron)

100% UO_2 in pellets : $d = 0.96$ cm

	Triang. Pitch			Square Pitch	
	VF = 0.6 1 b	VF = 0.5 2 b	VF = 0.4 3 b	VF = 0.5 4 b	VF = 0.4 5 b
1D-Cell *) k_{inf}	1.1028	1.1327	1.1243		
3D-Cell k_{inf}	1.0983	-	1.1276	1.1328	1.1221
ANISN **) k_{eff}	0.8627	0.8935	0.8921		

75% UO_2 in pellets : $d = 0.872$ cm

	Triang. Pitch			Square Pitch	
	VF = 0.6 1 d	VF = 0.5 2 d	VF = 0.4 3 d	VF = 0.5 4 d	VF = 0.4 5 d
1D-Cell *) k_{inf}	1.0777	1.1054	1.0935		
3D-Cell k_{inf}	1.0795	-	1.0937	1.1050	1.0914
ANISN **) k_{eff}	0.8435	0.8708	0.8682		

50% UO_2 in pellets : $d = 0.762$ cm

	Triang. Pitch			Square Pitch	
	VF = 0.6 1 f	VF = 0.5 2 f	VF = 0.4 3 f	VF = 0.5 4 f	VF = 0.4 5 f
1D-Cell *) k_{inf}	1.0707	1.0981	1.0875		
3D-Cell k_{inf}	1.0732	-	1.0877	1.0978	1.0859
ANISN **) k_{eff}	0.8371	0.8644	0.8630		

*) values not dependent from lattice geometry

**) homogenized cell cross-sections from the 1D-Cell calculations are used

Table 2 : k-infinity and $\Delta\rho$ values
for Benchmark Exercise 20
(1500 ppm Boron)

	k-infinity		$\Delta\rho$ [pcm]	
	VF = 0.4	VF = 0.6	VF = 0.4	VF = 0.6
IKE				
CGM/JEF-1	100%	1.12427	1.10284	0 0
	75%	1.09345	1.07768	2507 2117
	50%	1.08746	1.07074	3011 2718
	25%	1.08381	1.06738	3320 3012
	0%	1.08153	1.06551	3515 3177
FRANCE/CEAREF				
APOLLOREF	100%	1.12101	1.10081	0 0
	75%	1.08936	1.07732	2592 1981
	50%	1.08393	1.07042	3052 2579
	25%	1.08042	1.06670	3351 2905
	0%	1.07811	1.06512	3550 3044

Table 3

EXERCISE 20 : CASE 1b (100 % UO₂ in .962 cm . diam pellets, 0 % in solution, UO₂ cell fraction 0.6)

REACTION RATES	REGION 1 (UO ₂ PELLETS)				REGION 2 (UO ₂ + H ₂ O + B SOLUTION)			
	FAST	EPI-THERM	THERMAL ^{*)}	TOTAL ^{+)†}	FAST	EPI-THERM	THERMAL	TOTAL
CAPTURE $\Sigma_c^G \cdot \theta^G \cdot v$	²³⁵ U	2.6959E-3	4.3982E-2	5.1804E-2	9.8482E-2			
	²³⁸ U	5.6306E-2	2.7268E-1	5.7626E-1	3.8662E-1			
	¹⁶ O	2.8975E-3	1.8783E-6	7.6639E-6	2.9804E-3	1.2933E-3	8.7420E-7	3.8217E-6
	H					6.4970E-5	3.2587E-3	1.4254E-2
FISSION $\Sigma_f^G \cdot \theta^G \cdot v$	²³⁵ U	1.2757E-2	8.9442E-2	2.9244E-1	3.9465E-1			
	²³⁸ U	5.0096E-2	1.5200E-5	6.8126E-8	5.0295E-2			
	²³⁵ U	3.2329E-2	2.1794E-1	7.1259E-1	9.6289E-1			
	PRODUCTION $(\nu \Sigma_f)^G \cdot \theta^G \cdot v$ ²³⁸ U	1.4029E-1	3.5258E-5	1.5802E-7	1.4107E-1			

+) $E_{max} = 14.92$ MeV*) $E_{min} = 1.0E-5$ eV

Table 4

EXERCISE 20 : CASE 3b (100 % UO₂ in .962 cm . diam pellets, 0 % in solution, UO₂ cell fraction 0.4)

REACTION RATES	REGION 1 (UO ₂ PELLETS)				REGION 2 (UO ₂ + H ₂ O + B SOLUTION)			
	FAST	EPI-THERM	THERMAL *)	TOTAL +)	FAST	EPI-THERM	THERMAL	TOTAL
CAPTURE $\Sigma_c^{G,\theta} G.v$	²³⁵ U	1.3213E-3	2.6064E-2	6.3595E-2	9.0980E-2			
	²³⁸ U	2.8141E-2	1.7897E-1	7.0155E-2	2.7726E-1			
	¹⁶ O	1.9130E-3	1.1620E-6	9.3811E-6	1.9762E-3	1.8834E-3	1.2215E-6	1.0765E-5
	H					7.2329E-5	4.5534E-3	4.0151E-2
FISSION $\Sigma_f^{G,\theta} G.v$	²³⁵ U					2.3933E-4	1.2998E-2	1.1484E-1
	²³⁸ U	6.7511E-3	5.2574E-2	3.6508E-1	4.2441E-1			
		3.1983E-2	8.0053E-6	8.3173E-8	3.2123E-2			
PRODUCTION $(\nu \Sigma_p)^{G,\theta} G.v$	²³⁵ U	1.7228E-2	1.2811E-1	8.8959E-1	1.0350			
	²³⁸ U	8.9760E-2	1.8569E-5	1.9292E-7	9.0311E-2			

+) $E_{max} = 14.92$ MeV*) $E_{min} = 1.0E-5$ eV

Table 5

EXERCISE 20 : CASE 1f (50 % UO₂ in .762 cm . diam pellets, 50 % in solution, UO₂ fraction in H₂O 0.429)

REACTION RATES	REGION 1 (UO ₂ PELLETS)				REGION 2 (UO ₂ + H ₂ O + B SOLUTION)				
	FAST	EPI-THERM	THERMAL ^{*)}	TOTAL ^{†)}	FAST	EPI-THERM	THERMAL	TOTAL	
CAPTURE $\Sigma_C^{G,\bullet} G.v$	²³⁵ U	1.3932E-3	2.1999E-2	2.4119E-2	4.7511E-2	1.3362E-3	2.2223E-2	2.5264E-2	4.8823E-2
	²³⁸ U	2.9440E-2	1.1832E-1	2.6860E-2	1.7460E-1	2.8171E-2	1.7807E-1	2.8051E-2	2.3428E-1
	O	1.5175E-3	9.2811E-7	3.5701E-6	1.5603E-3	2.6840E-3	1.7452E-6	7.1236E-6	2.7607E-3
	H					6.4757E-5	3.0966E-3	1.2648E-2	1.5809E-2
	B _{nat}					2.1677E-4	8.8351E-3	3.6168E-2	4.5220E-2
FISSION $\Sigma_F^{G,\bullet} G.v$	²³⁵ U	6.6217E-3	4.4807E-2	1.3590E-1	1.8733E-1	6.2702E-3	4.4654E-2	1.4261E-2	1.9355E-1
	²³⁸ U	2.6259E-2	7.7232E-6	3.1744E-8	2.6363E-2	2.2431E-2	8.0292E-6	3.3165E-8	2.4404E-2
PRODUCTION $(\nu \Sigma_F)^{G,\bullet} G.v$	²³⁵ U	1.6786E-2	1.0918E-1	3.3114E-1	4.5713E-1	1.5883E-2	1.0882E-1	3.4750E-1	4.7222E-1
	²³⁸ U	7.3530E-2	1.7915E-5	7.3631E-8	7.3936E-2	6.8067E-2	1.8625E-5	7.6925E-8	6.8445E-2

+) $E_{max} = 14.92$ MeV*) $E_{min} = 1.0E-5$ eV

Table 6

EXERCISE 20 : CASE 3f (50 % UO₂ in .762 cm . diam pellets, 50 % in solution, UO₂ fraction in H₂O 0.25)

REACTION RATES	REGION 1 (UO ₂ PELLETS)				REGION 2 (UO ₂ + H ₂ O + B SOLUTION)				
	FAST	EPI-THERM	THERMAL ^{*)}	TOTAL ^{†)}	FAST	EPI-THERM	THERMAL	TOTAL	
CAPTURE $\Sigma_c^G \cdot \theta^G \cdot v$	²³⁵ U	6.7777E-4	1.2881E-2	2.9279E-2	4.2837E-2	6.5050E-4	1.3336E-2	3.1673E-2	4.5659E-2
	²³⁸ U	1.4555E-2	7.5146E-2	3.2320E-2	1.2202E-1	1.3915E-2	1.4263E-1	3.4859E-2	1.9140E-1
	¹⁶ O	1.0111E-3	5.6473E-7	4.3203E-6	1.0437E-3	2.7904E-3	1.7214E-6	1.4211E-5	2.8835E-3
	H					7.2258E-5	4.3116E-3	3.5614E-2	3.9998E-2
	B _{nat}					2.3913E-4	1.2307E-2	1.0186E-1	1.1441E-1
FISSION $\Sigma_f^G \cdot \theta^G \cdot v$	²³⁵ U	3.5026E-3	2.5991E-2	1.6788E-1	1.9738E-1	3.2765E-3	2.6398E-2	1.8192E-1	2.1159E-1
	²³⁸ U	1.6926E-2	4.0360E-6	3.8311E-8	1.6999E-2	1.5270E-2	4.3525E-6	4.1335E-8	1.5337E-2
PRODUCTION $(\nu \Sigma_f)^G \cdot \theta^G \cdot v$	²³⁵ U	8.9451E-3	6.3331E-2	4.0907E-1	4.8136E-1	8.3551E-3	6.4323E-2	4.4328E-1	5.1597E-1
	²³⁸ U	4.7498E-2	9.3620E-6	8.8862E-8	4.7788E-2	4.2862E-2	1.0096E-5	9.5877E-8	4.3128E-2

+) $E_{max} = 14.92$ MeV*) $E_{min} = 1.0E-5$ eV

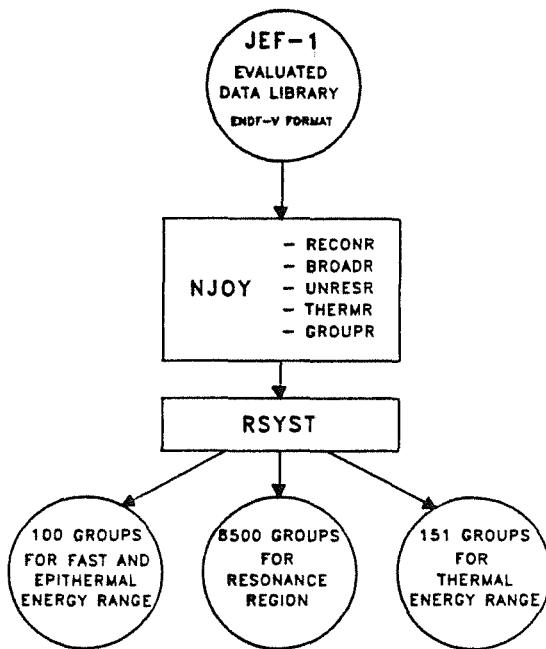


Figure 1: Generation of multigroup cross-section libraries for calculation of thermal fission systems

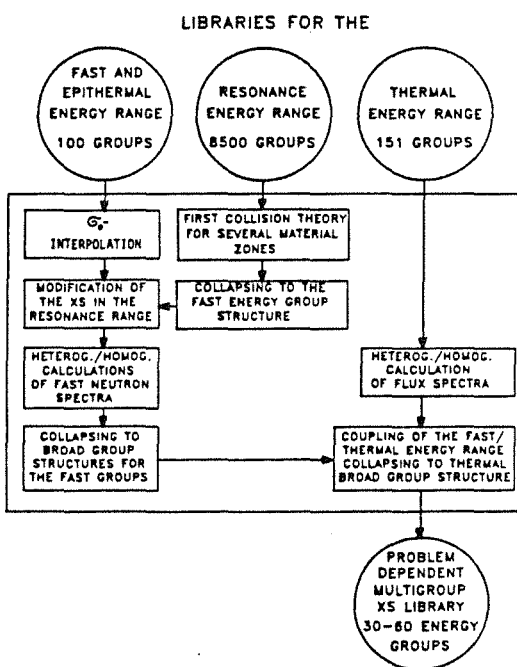


Figure 2: The RSYST/CGM module for cross-section processing for thermal reactor calculations

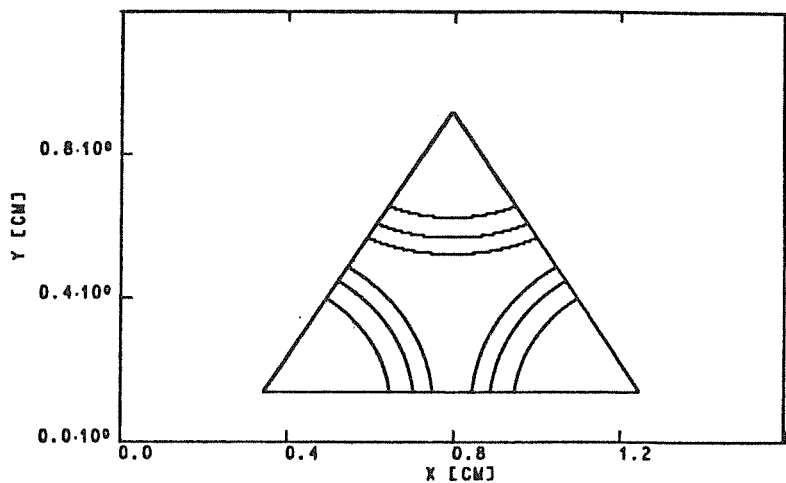


Figure 3: Geometry for tetraedric cell (z-Plane)

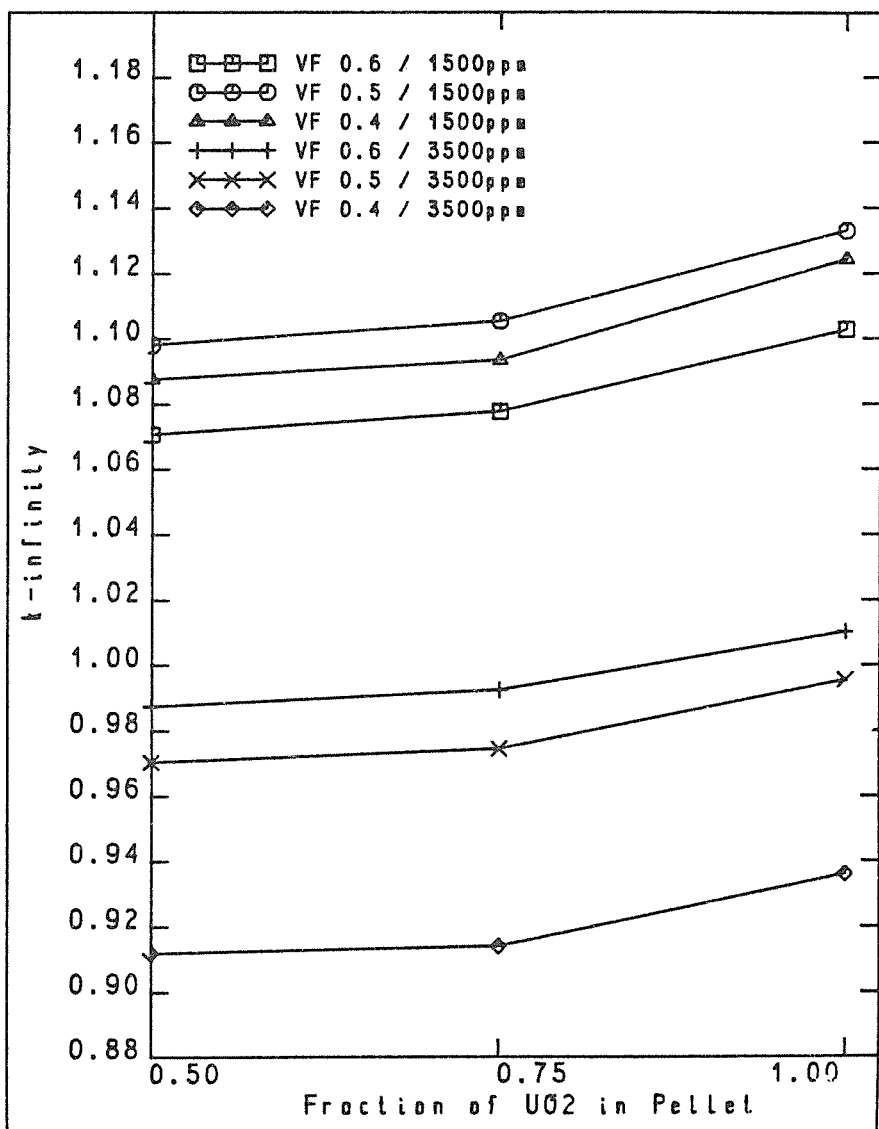


Figure 4: k -infinity for the Benchmark 20 as a function of UO_2 in pellets
(CGM/JEF-1)

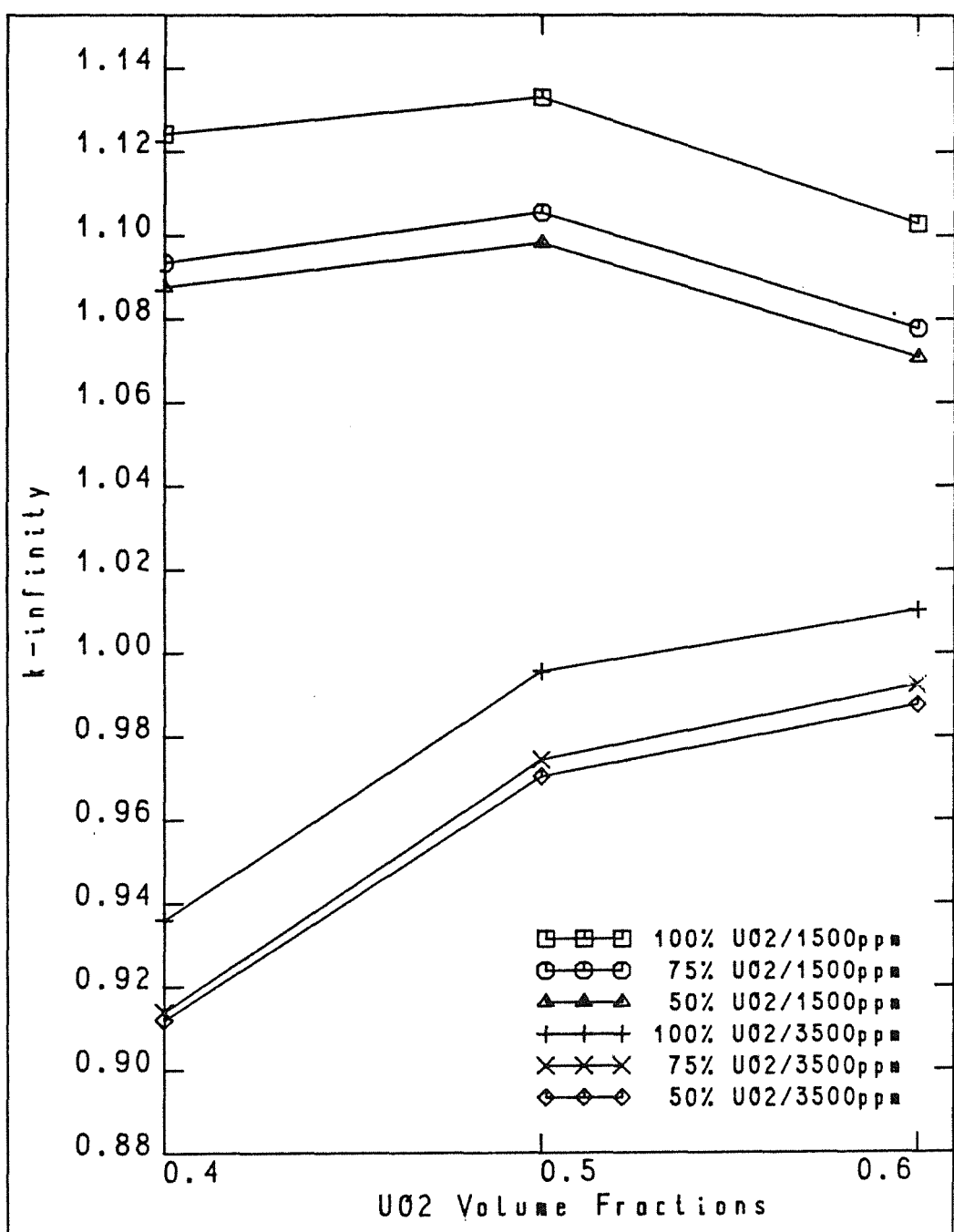


Figure 5: k-infinity for the Benchmark 20 as a function of UO₂ volume fraction
(CGM/JEF-1)

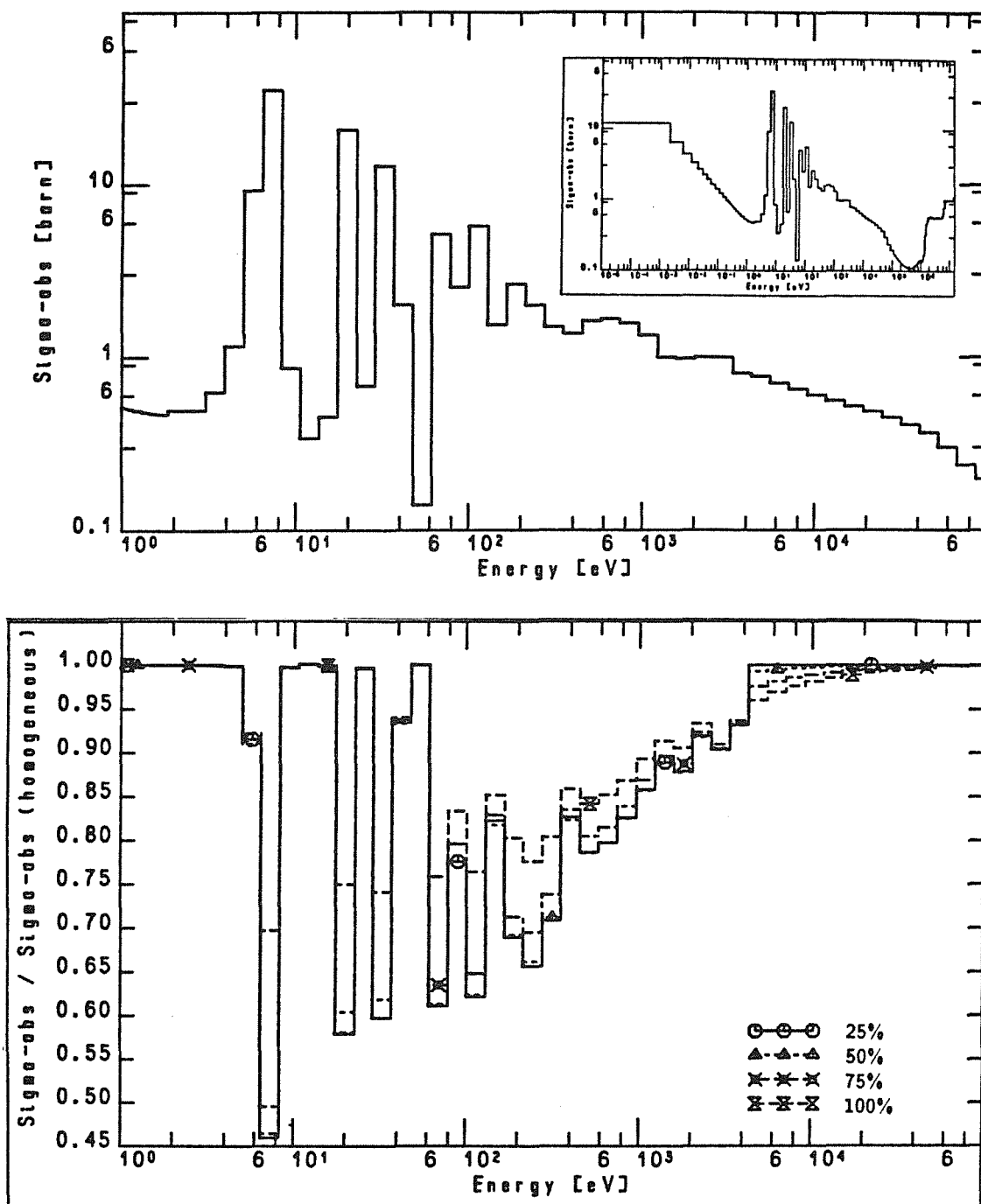


Figure 6: Relation between weighted U-238 multigroup-absorption cross-sections (GAM-II + LASER structure) for 25%, 50%, 75% and 100% UO_2 in pellet and cross-sections for the homogeneous case (0%).
 $V_f = 0.4, 1500 \text{ ppm, pellet zone}$

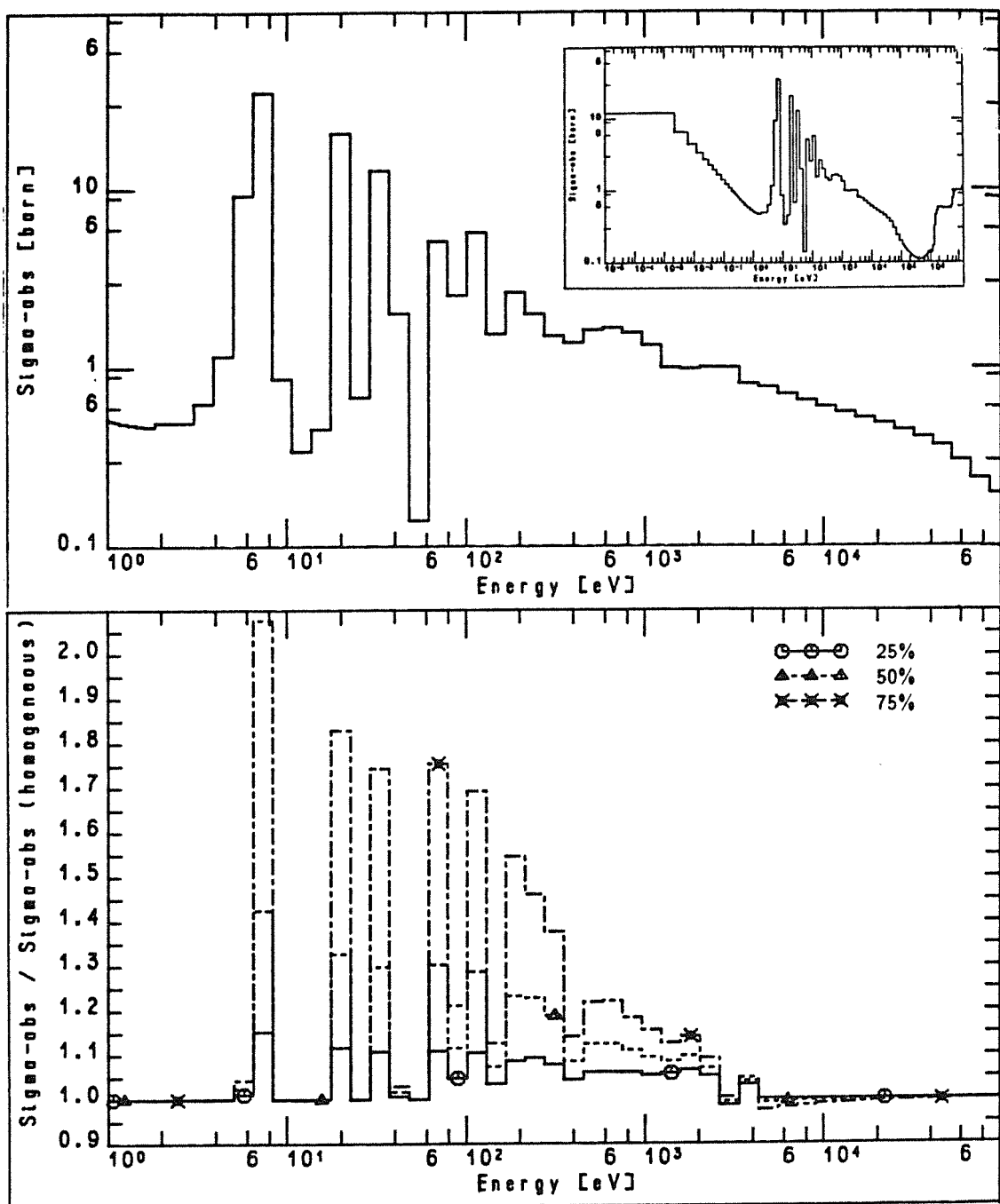


Figure 7: Relation between weighted U-238 multigroup-absorption cross-sections (GAM-II + LASER structure) for 25%, 50% and 75% UO_2 in pellet and cross-sections for the homogeneous case (0%).
Vf = 0.4, 1500 ppm, borated water + UO_2 zone

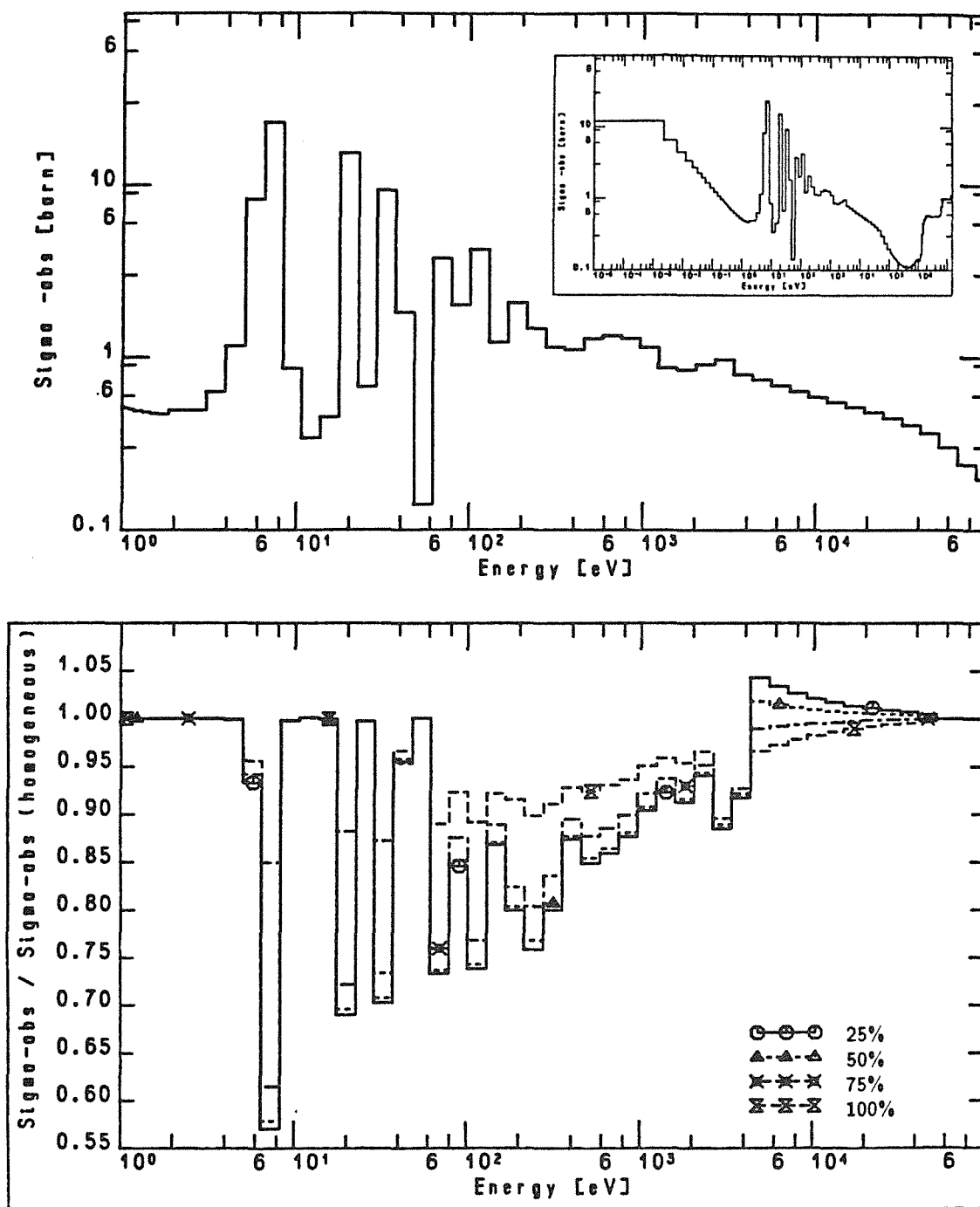


Figure 8: Relation between weighted U-238 multigroup-absorption cross-sections (GAM-II + LASER structure) for 25%, 50%, 75% and 100% UO_2 in pellet and cross-sections for the homogeneous case (0%).
Vf = 0.6, 1500 ppm, pellet zone

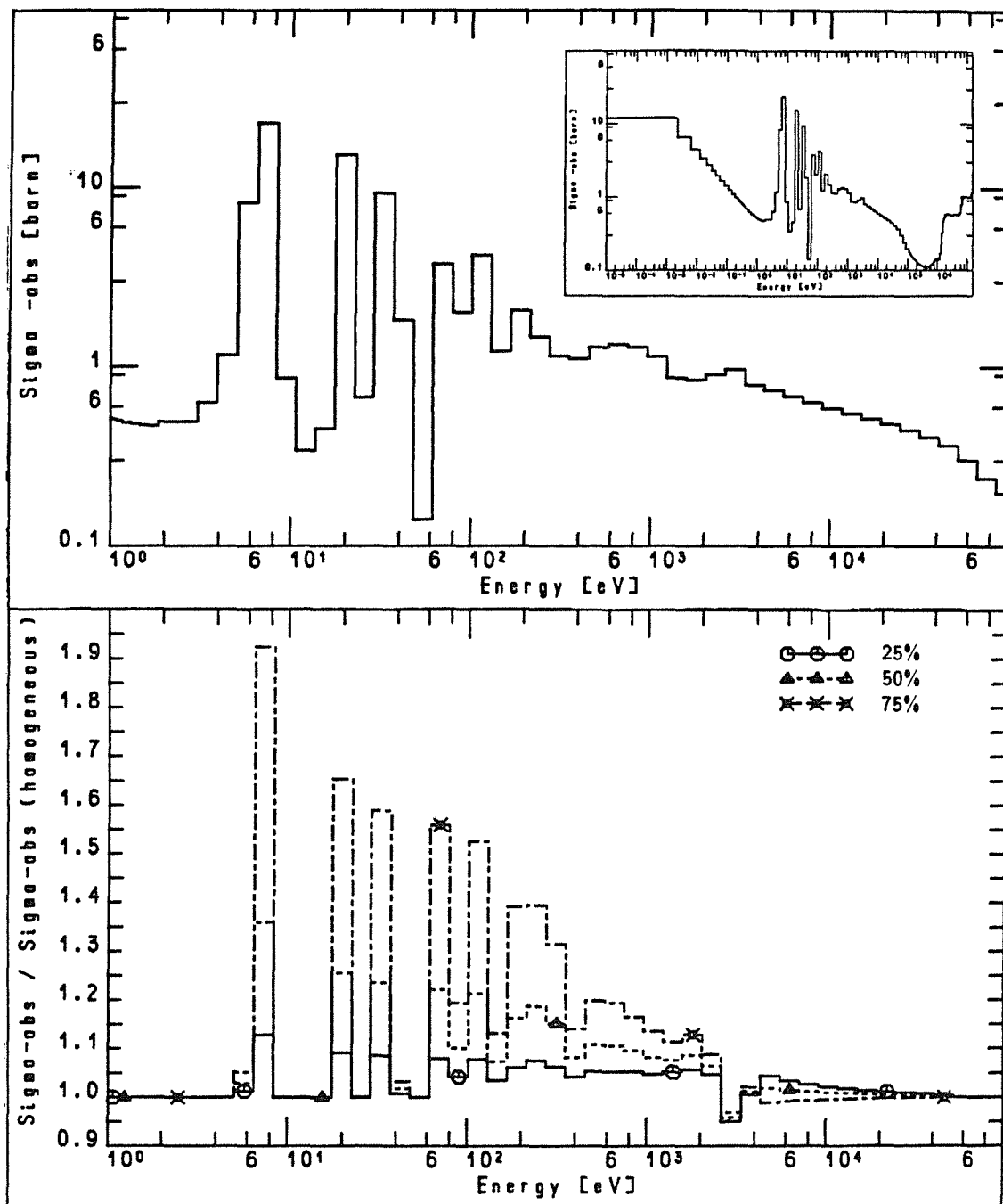


Figure 9: Relation between weighted U-238 multigroup-absorption cross-sections (GAM-II + LASER structure) for 25%, 50% and 75% UO_2 in pellet and cross-sections for the homogeneous case (0%).
Vf = 0.6, 1500 ppm, borated water + UO_2 zone

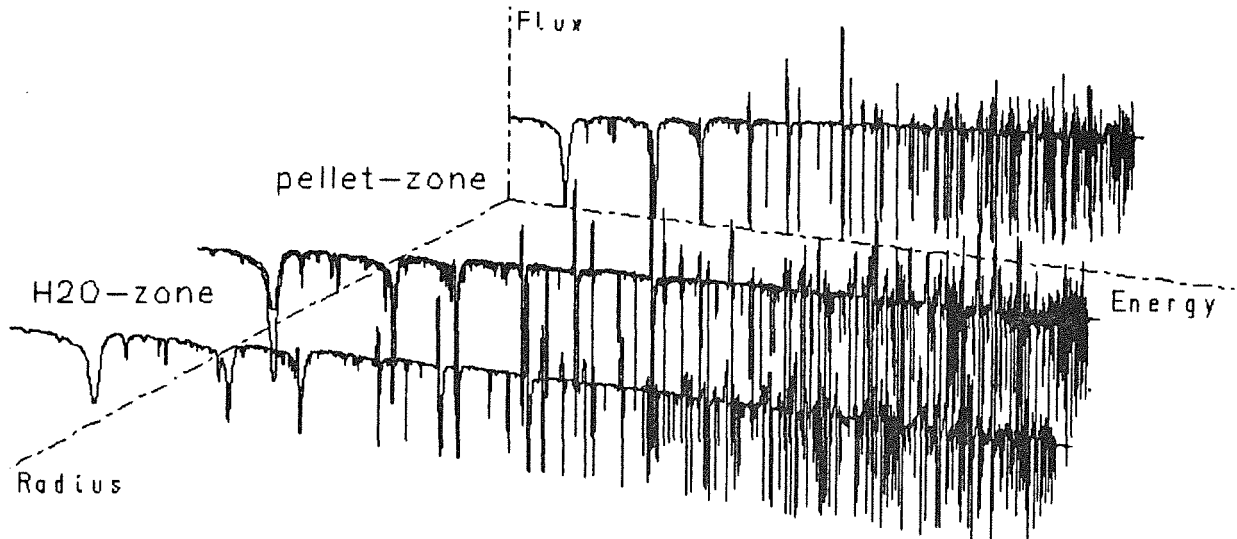


Figure 10: Neutron flux spectra in the pellet and water zone (100% UO_2 , $vf=0.4$, 1500 ppm)

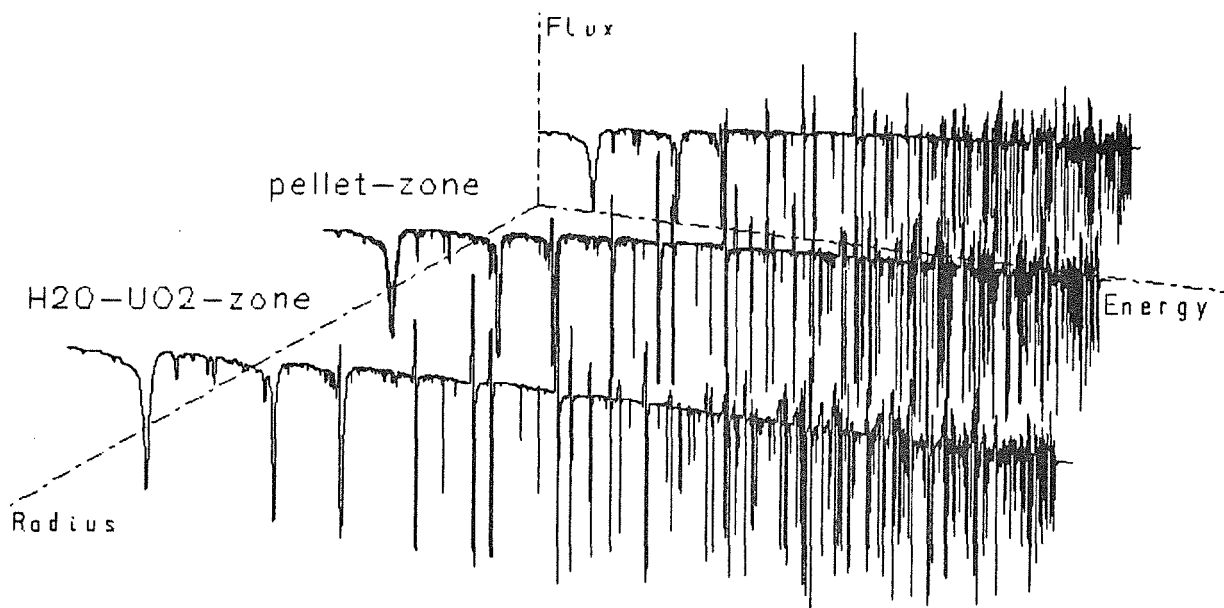


Figure 11: Neutron flux spectra in the pellet and water (+ UO_2) zone (50% UO_2 , $vf=0.4$, 1500 ppm)

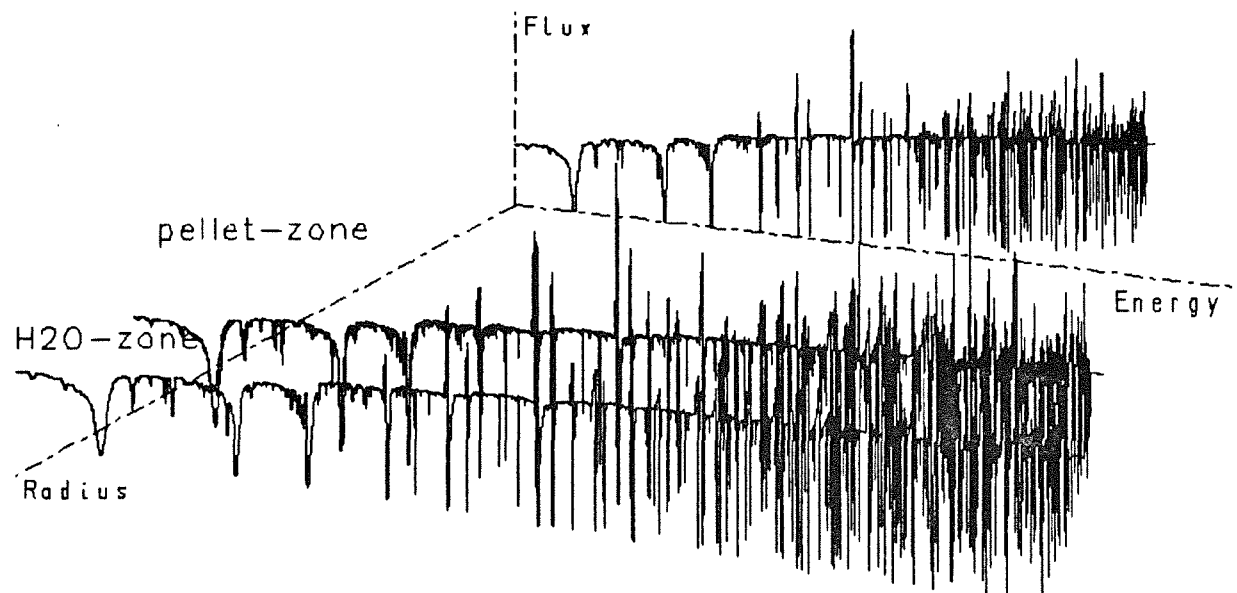


Figure 12: Neutron flux spectra in the pellet and water zone (100% UO_2 , $vf=0.6$, 1500 ppm)

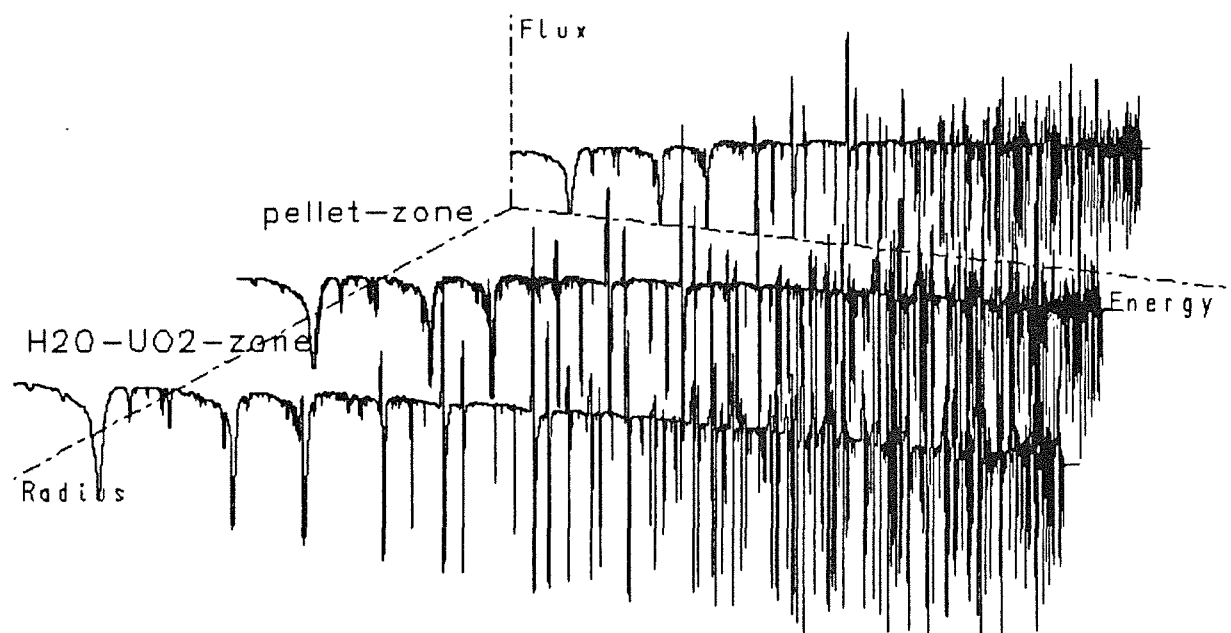


Figure 13: Neutron flux spectra in the pellet and water (+ UO_2) zone (50% UO_2 , $vf=0.6$, 1500 ppm)

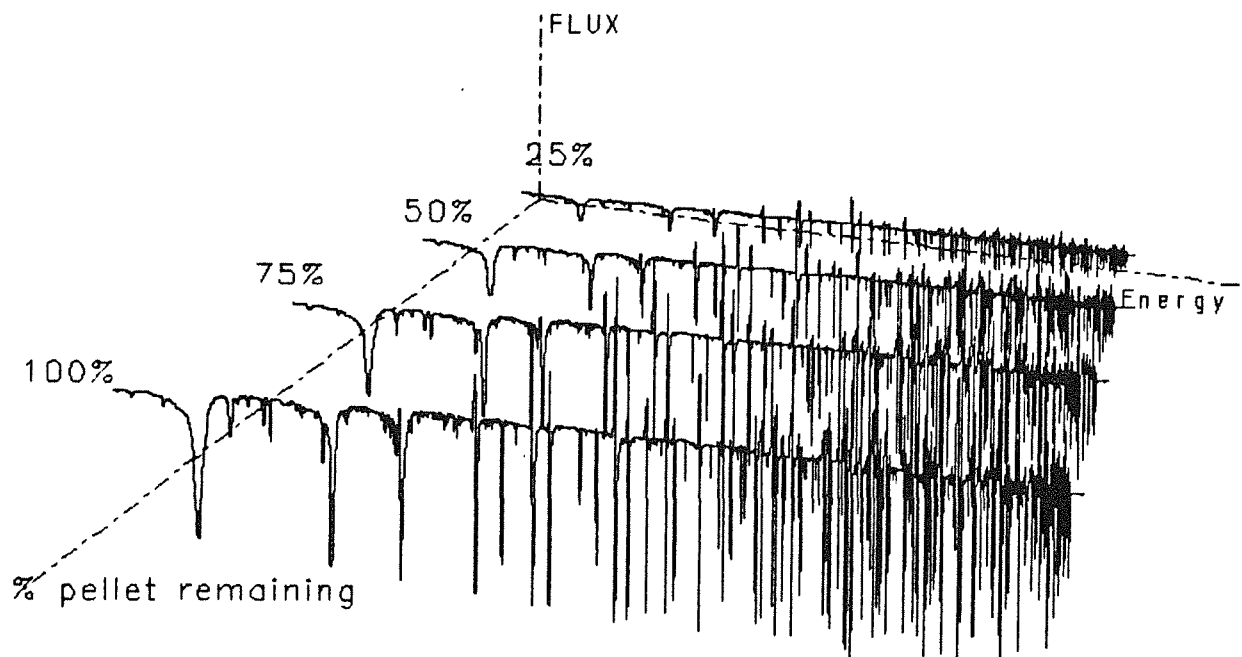


Figure 14: Neutron flux spectra as a function of pellet remaining ($vf=0.4$, 1500 ppm, pellet zone)

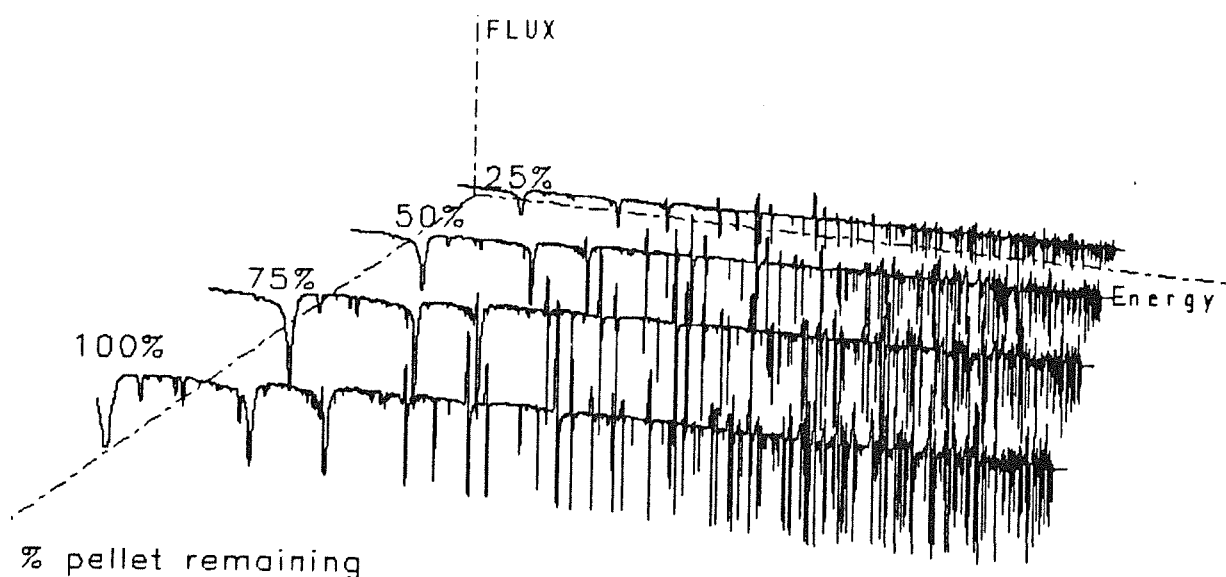


Figure 15: Neutron flux spectra as a function of pellet remaining ($vf=0.4$, 1500 ppm, moderator zone)

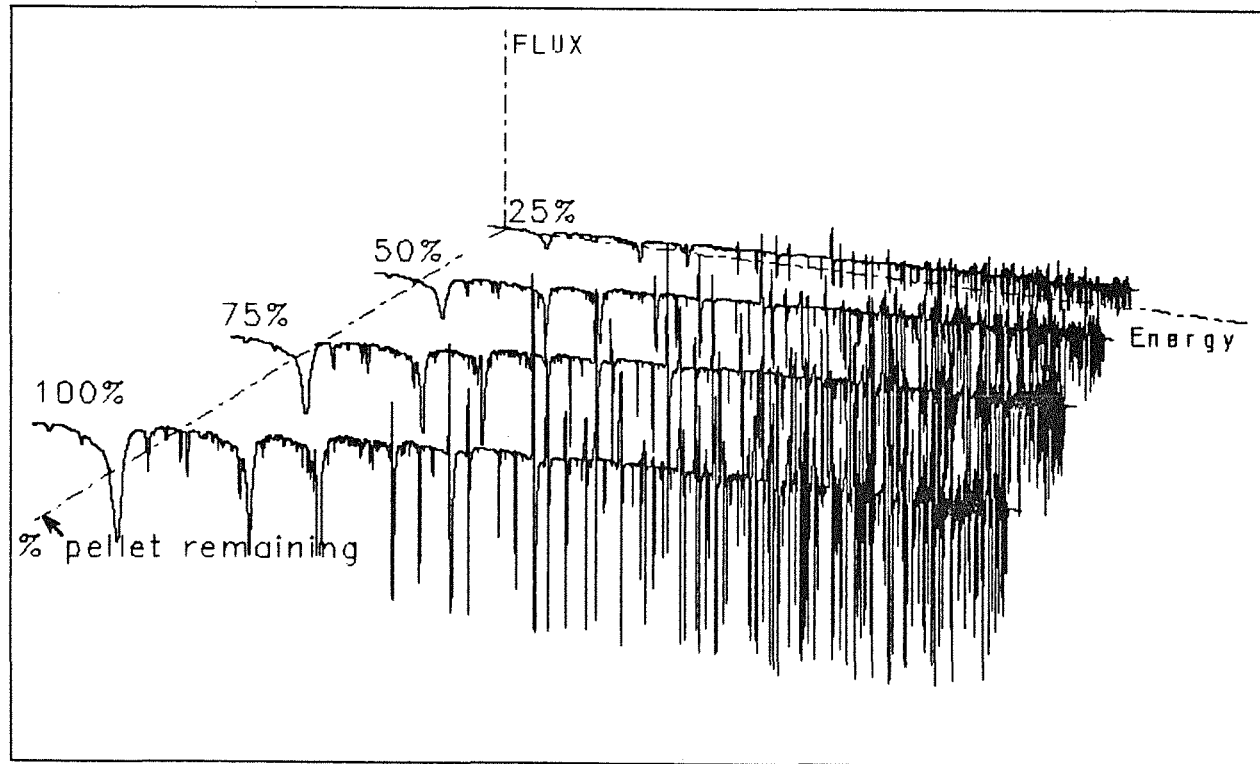
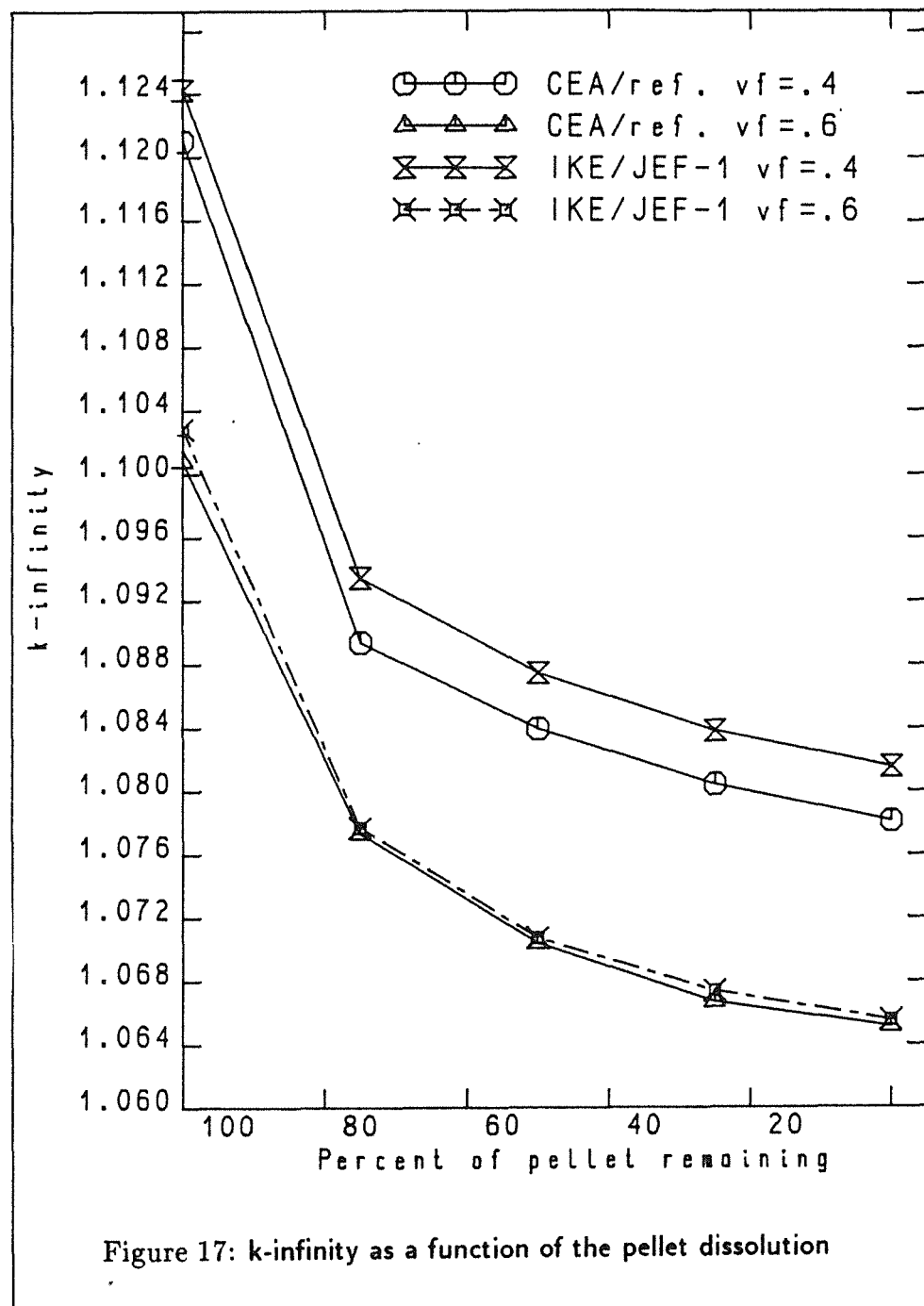
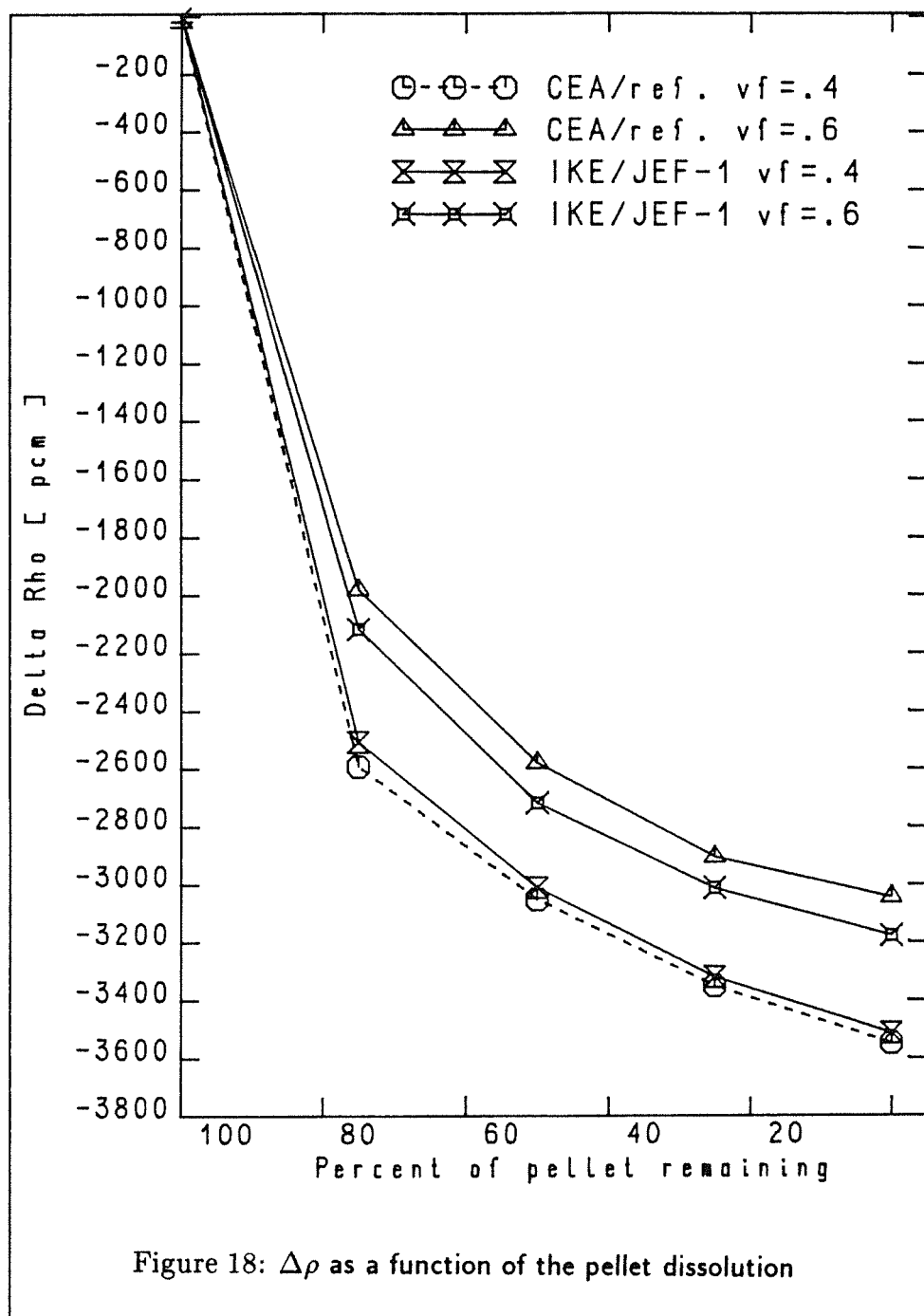
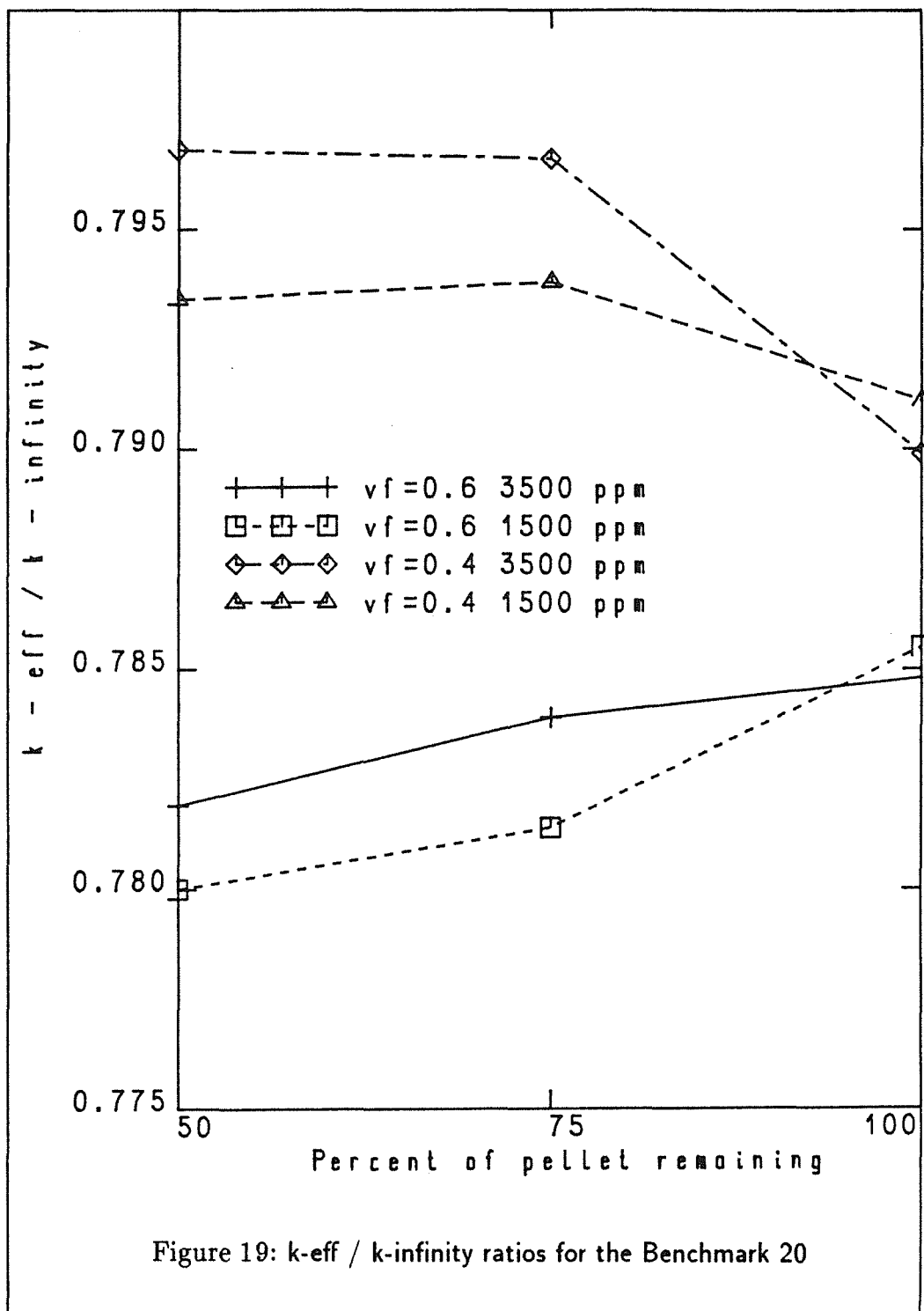


Figure 16: Neutron flux spectra as a function of pellet remaining ($vf=0.6$, 1500 ppm, pellet zone)







Annex

Specification of the Benchmark No. 20 of the OECD/NEA Criticality Working Group

Problem Set Title: $\text{U}(2.5)\text{O}_2$ in Borated H_2O

General Description: Square and triangular pitch lattices, Figures 1 & 2, of $\text{U}(2.5)\text{O}_2$ spherical pellets suspended in borated water and borated water- UO_2 slurries. Lattice materials in one-dimensional cylindrical geometry, Figure 3, reflected by 30 cm of water.

Pellet Diameters: 0.960 cm (full); 0.872 cm (3/4); 0.762 cm (1/2)

Boron Levels: 3500, 1500 WPPM

UO_2 Volume Fractions: Square Pitch - 0.5, 0.4
Triangular Pitch - 0.6, 0.5, 0.4

Temperature: 293 K, all materials

Atom Densities: Attached

Lattice Descriptions: Attached

Desired Results: k_{∞} for 30 lattice cells;
 k_{eff} for 30 water-reflected systems.

Set 1: All UO_2 in 0.96 cm dia. Pellet

<u>Case</u>	<u>Lattice Type</u>	<u>UO_2 Cell Fraction</u>	<u>Lattice Pitch (cm)</u>	<u>Boron (WPPM)</u>	<u>k_{∞}</u>	<u>k_{eff}</u>
1a	Triangular	0.6	1.0297	3500		
1b	"	0.6	1.0297	1500		
2a	"	0.5	1.0943	3500		
2b	"	0.5	1.0943	1500		
3a	"	0.4	1.1758	3500		
3b	"	0.4	1.1758	1500		
4a	Square	0.5	0.9749	3500		
4b	"	0.5	0.9749	1500		
5a	"	0.4	1.0501	3500		
5b	"	0.4	1.0501	1500		

Set 2: 75% UO_2 in 0.872 cm dia. Pellets
25% UO_2 in Borated Water

<u>Case</u>	<u>Lattice Pitch (cm)</u>	<u>Boron (wppm)</u>	<u>UO_2 Fraction in Water</u>	<u>Water & Boron Fractions</u>	<u>k</u>	<u>k_{eff}</u>
1c	1.0297(T)	3500	0.273		0.727	
1d	"	1500	"		"	
2c	1.0943(T)	3500	0.2		0.8	
2d	"	1500	"		"	
3c	1.1768(T)	3500	0.143		0.857	
3d	"	1500	"		"	
4c	0.9749(S)	3500	0.2		0.8	
4d	"	1500	"		"	
5c	1.0501(S)	3500	0.143		0.857	
5d	"	1500	"		"	

Set 3: 50% DO_2 in 0.762 cm dia. Pellet
50% DO_2 in Borated Water

<u>Case</u>	<u>Lattice Pitch (cm)</u>	<u>Boron (wppm)</u>	<u>UO_2 Fraction in Water</u>	<u>Water & Boron Fractions</u>	<u>k</u>	<u>k_{eff}</u>
1e	1.0297(T)	3500	0.429		0.571	
1f	"	1500	"		"	
2e	1.0943(T)	3500	0.333		0.667	
2f	"	1500	"		"	
3e	1.1768(T)	3500	0.25		0.75	
3f	"	1500	"		"	
4e	0.9749(S)	3500	0.333		0.667	
4f	"	1500	"		"	
5e	1.0501(S)	3500	0.25		0.75	
5f	"	1500	"		"	

Atom Densities ($\frac{\text{atoms}}{\text{bn-cm}}$)

Pellet (All Cases)

$$N(^{235}\text{U}) = 6.189 \cdot 10^{-4}; N(^{238}\text{U}) = 2.383 \cdot 10^{-2}; N(\text{O}) = 4.890 \cdot 10^{-2}.$$

Moderator, $\text{H}_2\text{O} + \text{B} + \text{DO}_2$

<u>Case</u>	<u>$N(\text{H})$</u>	<u>$N(\text{O})$</u>	<u>$N(^{10}\text{B})$</u>	<u>$N(^{11}\text{B})$</u>	<u>$N(^{235}\text{U})$</u>	<u>$N(^{238}\text{U})$</u>
1a through 5a	$6.676 \cdot 10^{-2}$	$3.338 \cdot 10^{-2}$	$3.854 \cdot 10^{-5}$	$1.565 \cdot 10^{-4}$	-	-
1b through 5b	$6.676 \cdot 10^{-2}$	$3.338 \cdot 10^{-2}$	$1.652 \cdot 10^{-5}$	$6.706 \cdot 10^{-5}$	-	-
1c	$4.853 \cdot 10^{-2}$	$3.762 \cdot 10^{-2}$	$2.802 \cdot 10^{-5}$	$1.137 \cdot 10^{-4}$	$1.690 \cdot 10^{-4}$	$6.506 \cdot 10^{-3}$
1d	$4.853 \cdot 10^{-2}$	$3.762 \cdot 10^{-2}$	$1.201 \cdot 10^{-5}$	$4.875 \cdot 10^{-5}$	$1.690 \cdot 10^{-4}$	$6.506 \cdot 10^{-3}$

2c and 4c	5.341-2	3.646-2	3.083-5	1.252-4	1.238-4	4.766-3
2d and 4d	5.341-2	3.648-2	1.321-5	5.364-5	1.238-4	4.766-3
3c and 5c	5.721-2	3.560-2	3.303-5	1.341-4	8.850-5	3.408-3
3d and 5d	5.721-2	3.560-2	1.416-5	5.747-5	8.850-5	3.408-3
1e	3.812-2	4.004-2	2.201-5	8.934-5	2.655-4	1.022-2
1f	3.812-2	4.004-2	9.431-6	3.829-5	2.655-4	1.022-2
2e and 4e	4.453-2	3.655-2	2.571-5	1.044-4	2.061-4	7.936-3
2f and 4f	4.453-2	3.655-2	1.102-5	4.473-5	2.061-4	7.936-3
3e and 5e	5.007-2	3.726-2	2.891-5	1.173-4	1.547-4	5.958-3
3f and 5f	5.007-2	3.726-2	1.239-5	5.029-5	1.547-4	5.958-3

Water Reflector

$$N(H) = 6.676-2; N(O) = 3.338-2.$$

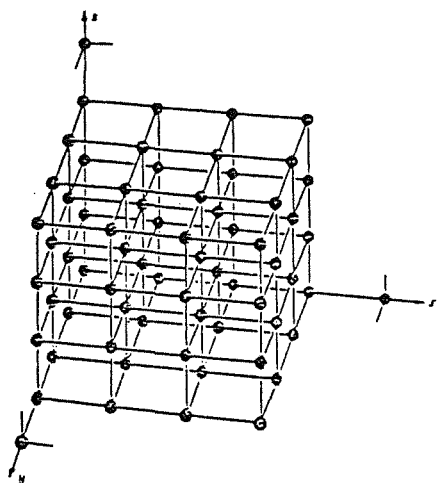


Fig. 1. Square Pitch, Cubic Cell, Infinite Lattice

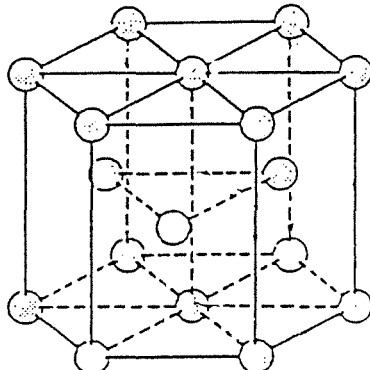


Fig. 2. Triangular Pitch, Dodecahedral Cell, Infinite Lattice

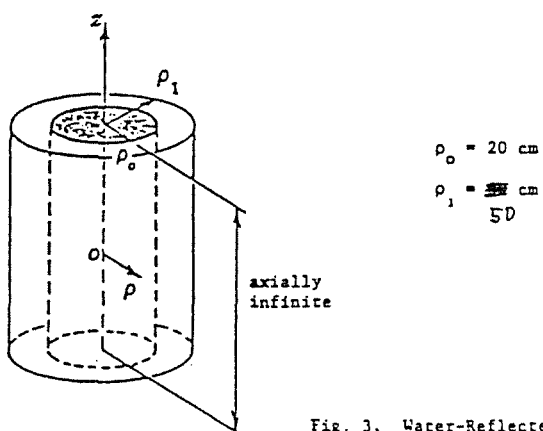


Fig. 3. Water-Reflected Cylinder of Lattice Material